Development of a hardware-in-the-loop test rig for testing turbogenerator waste heat recovery systems

Noam Olshina[1], Chris Manzie[1], Michael Brear[1], Peter Hield[2], Owen Tregenza[2]
1 The University of Melbourne, Vic, Australia
2 Defence Science and Technology, Vic, Australia
nolshina@student.unimelb.edu.au

ABSTRACT

The overall energy efficiency of maritime platforms is increasingly important, for both commercial and military applications. This research project focuses on recovering some of the energy lost through the exhaust of a diesel engine using a turbocompounding system consisting of a radial flow turbine coupled to an electrical generator (turbogenerator). This system can be retrofitted to existing diesel engines and only marginally increases the engine weight, volume and complexity. Additionally, the reduced exhaust gas temperature reduces the vessel's thermal signature.

To gain a better understanding of the expected performance of the turbogenerator on a diesel engine, and the effectiveness of Model Predictive Control (MPC), the turbogenerator and MPC controller is tested in a test rig using Hardware-in-the-Loop (HIL) simulations. As opposed to simulation only based development, HIL simulations enable the testing and development of control systems under more realistic operating conditions. In this work, the test rig is used to subject the turbogenererator to realistic surface vessel and submarine operating conditions. This paper details the test rig used in this project, the performance mapping of the turbogenerator, the methodology used to reproduce engine operating conditions within the test rig, and the interface between the test rig and the simulation environment.

INTRODUCTION

Improving the energy efficiency of maritime vessels results in environmental, economic and for the military, strategic benefits [1].

WHR is a class of technologies for improving the energy efficiency of engines by targeting the energy contained in the exhaust gasses which would otherwise be wasted. Of the total energy contained in the fuel, approximately 40% is converted into useful work, 30% lost through the hot exhaust gasses and the remainder lost through other systems.

There are several Waste Heat Recovery (WHR) technologies in use and the subject of ongoing research [2]. The research presented in this paper focuses on turbocompounding, which involves the addition of a secondary power turbine (turbogenerator) in the exhaust stream of an engine. Turbocompounding provides competitive fuel efficiency gains compared to other WHR technologies with minimal increase in engine weight and complexity [2].

Diesel-electric submarines are required to operate at constant speed to minimise acoustic emissions, as well as maximise engine reliability and longevity. This has been difficult to achieve in practice. Air is drawn through a snorkel mast and exhausted underwater through the hull. This results in a low engine intake air pressure and a high and varying exhaust back pressure as ocean waves pass over the submarine (Figure 1). Consequently, the engine experiences high and varying exhaust gas temperatures and engine speed fluctuations,

increasing engine wear and reduced reliability, resulting in a demanding maintenance schedule [3].

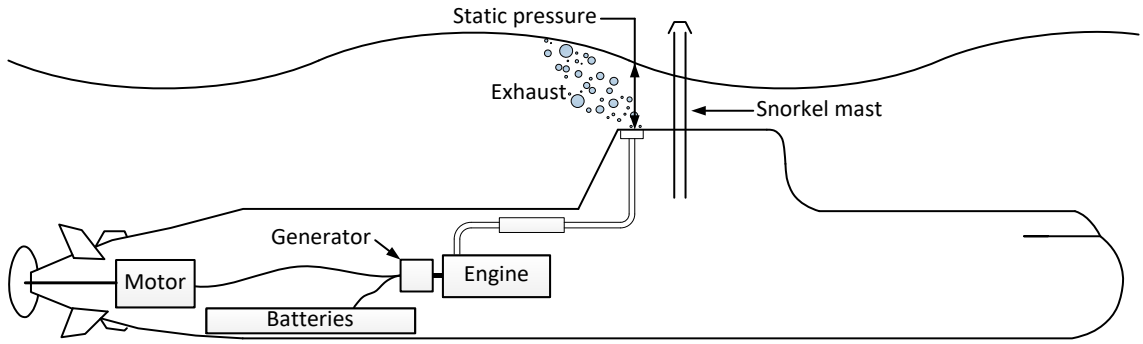

Figure 1: Schematic diagram illustrating how ocean waves cause engine back-pressure fluctuations.

Naval surface vessel engines are required to provide a variable power output consisting of the hotel load and propulsive power demand. They must also respond to changes in demand quickly to meet mission objectives. In doing so, the engine operates over a large range of set points with a significant amount of time transitioning between these.

Unlike naval applications, commercial vessel powertrains are required to mostly operate at steady state, and without the challenges of the unique operating environment of submarine engines. Therefore, the expected performance and idiosyncrasies of commercially available marine turbocompounding systems, such as that developed by MAN Diesel & Turbo [4], operating in challenging naval environments are unknown. However, this commercial experience provides additional motivation for and guidance in exploring this form of WHR for naval applications, and ultimately the development of a suitable naval turbocompounding system.

To control the complex engine-turbogenerator system, model predictive control (MPC) offers attractive advantages compared to other control techniques. MPC allows for the fulfilment of multiple objectives simultaneously, while satisfying system constraints. These objectives may include maintaining engine speed, maximising power or minimising fuel use, all while ensuring specified engine operating limits are not exceeded. Constraints may also include emission constraints, which have regulated limits [1]. MPC is a novel control strategy for maritime engine control.

Previous work undertaken by Defence Science and Technology and the University of Melbourne explored the use of MPC to control submarine engines subjected to varying exhaust back pressure [5] as well as for fixed diesel engines [6]. These studies demonstrated the potential of MPC as a control solution for these applications, with distinct advantages over traditional PID control.

The current focus of research efforts is to experimentally determine the effectiveness of turbocompounding on naval submarines and surface vessels using an MPC control strategy. To accomplish this, the MPC controller will be tested by controlling a simulated engine coupled to the real turbogenerator and subjected to realistic operating conditions. This type of experiment is referred to as Hardware-in-the-Loop (HIL) testing.

HIL testing offers a number of advantages over alternative control system testing methodologies. Most importantly, since the engine is simulated, testing can be done safely without risk to personnel or damage to a real engine, especially when testing on the limits

of the engine's operational range. For the application here, the simulated engine, its configuration with the turbogenerator and the design of the MPC controller can all be modified with relative ease. This enables relatively inexpensive studies to determine the most suitable engine-turbogenerator configuration for a given application (eg: surface vessel vs. submarine), or to tune the various design parameters of the MPC formulation to improve the closed loop system performance.

For successful HIL testing, the turbogenerator test rig must be capable of reproducing realistic operating conditions and compensating for differences between the test rig and simulation environment. For MPC, an accurate model of the turbogenerator (and wastegate valve) is needed.

This paper begins by describing DST's test rig and a brief discussion of the MPC formulation. The main sections detail the development of the test rig control systems used to reproduce realistic operating conditions, the identification of the turbogenerator and wastegate valve performance maps needed for the MPC controller's internal system model, and the methodology used to interface the test rig with the simulation environment. The paper concludes by outlining the main results of this paper and the future work for this project.

TEST RIG

The DST test facility includes a test cell, air processing plant and an adjoining control room. The air processing plant can deliver air at pressures and mass flow rates comparable to the exhaust gas produced by the marine diesel engines. The test rig shown in Figure 2 is located in the test cell and is comprised of the turbogenerator system, hot air pipework, actuated valves, sensor and control network and control and data acquisition systems.

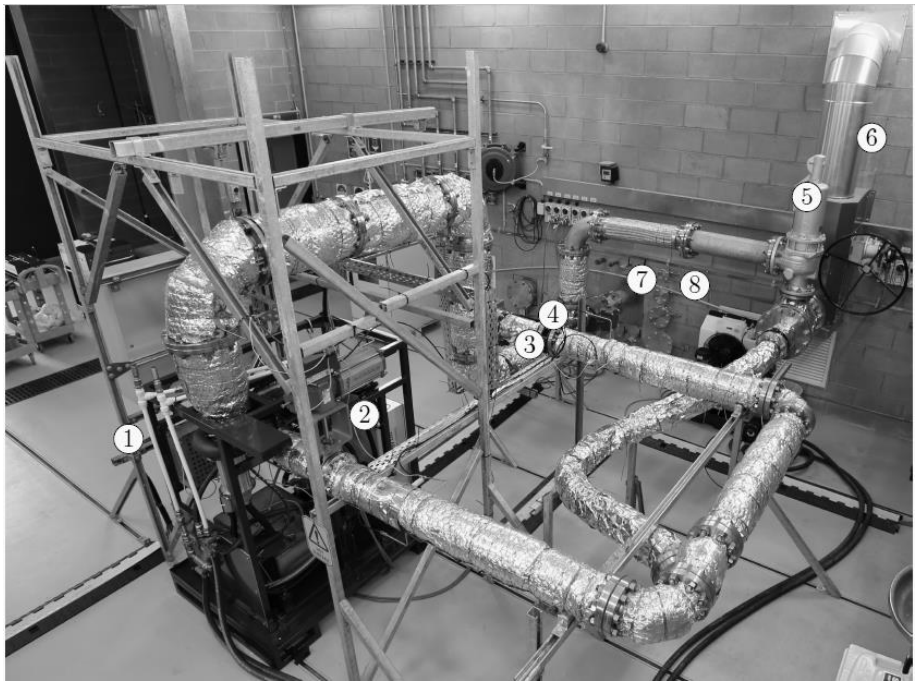

Figure 2: Photograph of test rig including: (1) turbogenerator system in dark frame, (2) actuated wastegate valve, (3) actuated bypass valve, (4) actuated back pressure valve (behind bypass valve), (5) pressure relief valve, (6) supply air pipe, (7) exhaust air pipe, (8) coolant radiator.

The turbogenerator system has been provided by Bluebox Energy Ltd. and includes the turbogenerator, actuated wastegate valve, water and oil cooling systems, power electronics, sensors and proprietary control system. The turbogenerator itself was manufactured by Bowman Power Group. It consists of a radial flow turbine directly coupled to a high speed 3 phase, 4 pole permanent magnet synchronous generator. The generator is rated for 60kW AC power output, with rotational speeds up to 55kRPM. Generated AC power is converted to DC and absorbed by the test facility's load bank. A proprietary control system is used to control the speed of the turbogenerator, either at a fixed speed setpoint or in 'maximum power' or 'maximum efficiency' modes.

In addition to the wastegate valve at the turbogenerator inlet, there are three actuated butterfly valves used to control the airflow throughout the rig. By controlling these valves appropriately, the operating conditions that the turbogenerator would be exposed to during service for both surface vessel and submarine applications can be reproduced. These valves include an inlet valve, turbogenerator bypass valve and back-pressure valve.

The inlet valve is used to reduce the pressure supplied by the air processing plant, so that in pressure in the volume upstream of the wastegate valve is approximately that of a marine diesel engine's exhaust. The bypass valve is controlled so that its upstream pressure follows an exhaust manifold reference pressure provided by the engine simulation. The back-pressure valve is used to reproduce the fluctuating exhaust back pressure typical of submarine operating conditions.

The test rig is fitted with a comprehensive sensor network used to measure the pressure and temperature at critical points within the test rig, as well as the mass flow rates through the turbogenerator and bypass lines. In addition to the sensors provided by Bluebox Energy Ltd. with the turbogenerator system, which transmit data over a CANBus, additional sensors have been added to independently measure the turbogenerator speed, generated DC voltage and DC current.

A LabVIEW system is used for data acquisition as well as to control of the valves and set the turbogenerator speed setpoint. A real-time dSPACE system is used as a platform to run the simulations of the engine in parallel with the MPC controller. Where required, data is transmitted between these two platforms using their analog inputs and outputs.

MODEL PREDICTIVE CONTROL

Model predictive control (MPC) techniques encompass a family of advanced control schemes which share defining characteristics. A mathematical model of a system to be controlled is used to determine the optimal sequence of inputs (and corresponding system states and outputs) along a fixed prediction horizon, while ensuring that system constraints are satisfied. The control input is determined using constrained optimisation techniques to find the minimum of a predefined cost function, which encapsulates the control objective. Interested readers are directed to [1] for a brief introduction into MPC and a selection of instructive references.

The MPC controller used in this work is a variant of standard MPC formulations known as Economic MPC (EMPC) and is based on the formulation presented in [7]. The main difference between standard MPC and EMPC is that the cost function explicitly penalises

economic criteria such as fuel consumption. For example, for submarine operation, the cost function is defined as

$$J_{\text{sub}} := \sum_{i=0}^{N-1} \alpha_1 \left(\omega_{\text{e}} - \omega_{\text{e,ref}}\right)^2 + \alpha_2 \left(T_{\text{ex}} - T_{\text{ex,ref}}\right)^2 + \alpha_3 \left(P_{\text{gen}} - P_{\text{gen,ref}}\right)^2 + \alpha_4 \dot{m}_{\text{f}}, \qquad (1)$$

where ω_{e} is the engine speed, T_{ex} is the exhaust gas temperature, P_{gen} is the sum of the power generated by the engine $P_{\text{gen,e}}$ and the turbogenerator $P_{\text{gen,tg}}$, and $\dot{m}_{\text{f}}$ is the fuel mass flow rate. Subscript $(\cdot)_{\text{ref}}$ is for a used defined reference values which may be set by an operator, α_1,…,α_4 are weights and N is the MPC prediction horizon length.

For surface vessel gensets where meeting power demand and maximising fuel efficiency are of primary interest, we can set the weights in (1) to be $\alpha_1 = \alpha_2 = 0$. Similarly for propulsion engines where the engine is directly coupled to the ship's propellers and engine speed and fuel efficiency are of importance, we set $\alpha_2 = \alpha_3 = 0$ in (1). In both cases, by explicitly penalising the fuel consumption, the fuel efficiency of the engine/turbogenerator system is maximised.

In designing the EMPC controller, there are numerous design parameters which affect both closed loop performance and the computational complexity of the controller. Selection of these design parameters to achieve the specified closed loop performance without over specifying the EMPC implementation hardware is a challenging problem [8]. Some of these parameters include EMPC controller's prediction horizon time, horizon length (N) and the fidelity of the mathematical model of the engine-turbogenerator system.

HARDWARE IN THE LOOP CONFIGURATION AND CONTROL

To include the turbogenerator within a HIL simulation, three aspect of the test rig control are considered:

1. Representation of the simulated engine operating conditions within the test rig, by using the test rig's inlet, bypass and back pressure valves.
2. Development of the turbogenerator and wastegate valve models for use within the EMPC controller's mathematical plant model.
3. The hot air supply system was originally designed to replicate compressor exit conditions for gas turbine engine and thus cannot replicate the temperatures typically seen in a diesel engine exhaust system. Additionally, this system is not capable of rapid changes in temperature typical of diesel exhaust systems during engine transients. Therefore, the difference in temperature between the simulated exhaust manifold temperature and the actual test rig gas temperature upstream of the wastegate valve must be considered and compensated for in the interaction between the test rig, the EMPC controller and the simulated engine. These aspects of the HIL simulation are described in the sections below.

Experimental techniques often make use of dimensional analysis to distill the seemingly complex relationship observed between variables into simple relationships between dimensionless groups of these variables. The methodology of finding suitable dimensionless groups which can be used to characterise complex system behaviour is well established and known as the Buckingham-Pi principle [9, Chapter 5], and is a technique used extensively in this work. For example, to derive a mathematical model of the

turbogenerator for use within the EMPC controller, which can be used for varying turbogenerator inlet pressures and temperatures.

Relevant dimensionless quantities are first derived using the Buckingham-Pi principle with the dimensioned variables of mass flow $\dot{m}$, speed ω, power P, pressure p and temperature T at the inlet $(\cdot)_{\text{in}}$ and outlet $(\cdot)_{\text{out}}$, turbine diameter d_{tg} and specific heat capacities c_p and c_v. This results in the following dimensionless groups relevant for the turbogenerator and control valve mapping:

$$\Pi_{\text{tg}} = \frac{p_{\text{in}}}{p_{\text{out}}}, \qquad \text{M}_{\text{tg}} = \frac{\dot{m}_{\text{tg}}\sqrt{c_p T_{\text{in}}}}{d_{\text{tg}}^2 p_{\text{in}}}, \qquad \Omega_{tg} = \frac{d_{\text{tg}}\omega_{\text{tg}}}{\sqrt{c_p T_{\text{in}}}},$$
$$\text{T}_{\text{tg}} = \frac{T_{\text{in}}}{T_{\text{out}}}, \qquad BSR_{\text{tg}} = \frac{d_{\text{tg}}\omega_{\text{tg}}}{2\sqrt{2c_p T_{\text{in}}\left(1-\Pi_{\text{tg}}^{1-1/\gamma}\right)}}, \qquad \Upsilon_{tg} = \frac{P_{\text{tg}}}{d_{\text{tg}}^2 p_{\text{in}}\sqrt{c_p T_{\text{in}}}}. \tag{2}$$

where $\gamma = c_p/c_v$.

VALVE CHARACTERISATION AND CONTROL

The simulated engine operating conditions that must be reproduced within the test rig include the exhaust manifold pressure and, for the submarine operating condition, the wave induced back-pressure.

For the exhaust manifold pressure, the test rig's inlet valve is set to a fixed position to reduce the pressure supplied by the air processing plant to a pressure closer to the simulated exhaust manifold pressure. The bypass valve is then actively controlled so that its upstream pressure follows a reference exhaust manifold pressure provided by the engine simulation. As the control architecture for the bypass valve and the back-pressure valve are the same, the architecture will be illustrated using the back-pressure valve.

The back-pressure due to waves passing over the exhaust port of a submarine is reproduced by controlling the test rig's back pressure valve so that it's upstream pressure, p_{ex}, tracks a reference exhaust back-pressure, $p_{\text{ex,ref}}$. The reference back-pressure can be any suitable timeseries representative of ocean conditions that a submarine may encounter while snorting. These timeseries could be obtained from direct measurement on board a submarine, generated from wave spectra, or simply consist of a single sinusoidal waveform representative of a given sea state.

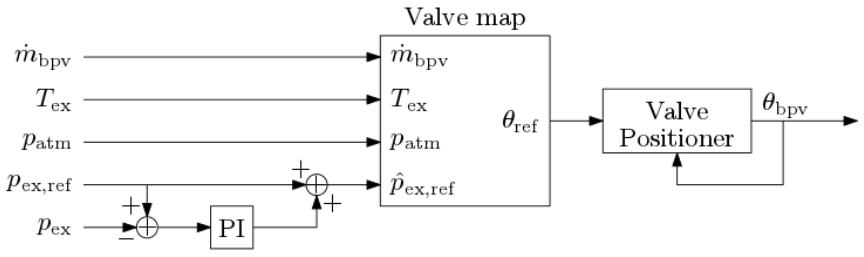

Figure 3: Back pressure valve control architecture.

Since the pressure ratio across a butterfly valve is a nonlinear function of valve angle and mass flow rate, a typical PID controller would struggle to reproduce the reference upstream pressure over the required operating range. Therefore, a model-based controller shown in

Figure 3 has been developed using a PI / feedforward architecture. A valve map is used to convert the back-pressure timeseries into a reference valve angle, which is then tracked by the valve's actuator. In addition, to the feedforward valve map, a PI controller is used to further reduce any error between p_{ex} and $p_{\mathrm{ex,ref}}$ and provides an augmented reference back-pressure, $\hat{p}_{\mathrm{ex,ref}}$ to the feedforward map. The valve positioner, which is integrated within the valve's actuator tracks θ_{ref}.

To develop the valve map, we model the valve as an isothermal orifice, considering the gas as a compressible fluid [10, Chapter 2]. Firstly, define the pressure ratio across the valve as $\Pi_{\mathrm{bpv}} = p_{\mathrm{atm}}/p_{\mathrm{ex}}$, where p_{atm} is the atmospheric. The mass flow rate through the valve is given by

$$\dot{m}_{\mathrm{bpv}} = A_{\mathrm{eff}}\left(\theta_{\mathrm{bpv}}\right)\frac{p_{\mathrm{ex}}}{\sqrt{RT_{\mathrm{ex}}}}\Psi(\Pi_{\mathrm{bpv}}), \tag{3}$$

where T_{ex} is the valve's upstream temperature,

$$\Psi(\Pi) := \begin{cases} 1/\sqrt{2}, & 0 < \Pi \leq 1/2 \\ \sqrt{2\Pi(1-\Pi)}, & 1/2 < \Pi < 1, \end{cases} \tag{4}$$

and $A_{\mathrm{eff}}\left(\theta_{\mathrm{bpv}}\right)$ combines the valve's coefficient of discharge and effective throat area into a single function of valve angle, θ_{bpv}. The map used in the feedforward controller is an inversion of (3) in the form $\theta_{\mathrm{ref}} = f\left(\dot{m}_{\mathrm{bpv}}, \hat{p}_{\mathrm{ex,ref}}, p_{\mathrm{atm}}, T_{\mathrm{ex}}\right)$.

A series of experiments was conducted to identify the form of $A_{\mathrm{eff}}\left(\theta_{\mathrm{bpv}}\right)$, by measuring $\dot{m}_{\mathrm{bpv}}$, p_{atm}, p_{ex}, T_{ex} and θ_{bpv} at operating points spanning the operating range of the valve. It was found that $A_{\mathrm{eff}}\left(\theta_{\mathrm{bpv}}\right)$ was well fitted by a quadratic function as seen in Figure 4.

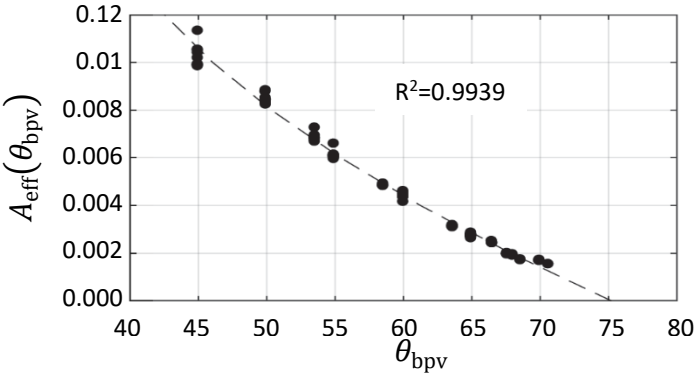

Figure 4: Back pressure valve characterisation

To validate the performance of the control architecture, and to tune the gains of the PI controller, the closed loop system was tested using a number of $p_{\mathrm{ex,ref}}$ signals, which were generated using a sinusoidal signal with amplitude and frequency corresponding to sea states 2 to 5. Figure 5 shows an 60 second extract from the generated $p_{\mathrm{ex,ref}}$ and measured p_{ex} for sea state 5. This extract indicates that the back pressure is well reproduced.

TURBOGENERATOR PERFORMANCE MAPPING

To determine the performance of the turbogenerator, experimental data was collected covering its entire operating range. Each datum represents data collected at 10kHz over 10 second intervals, and then averaged to reduce the impact of noise. Between operating

points, sufficient time was allowed for any transient dynamics to settle. In total, 301 data points were collected.

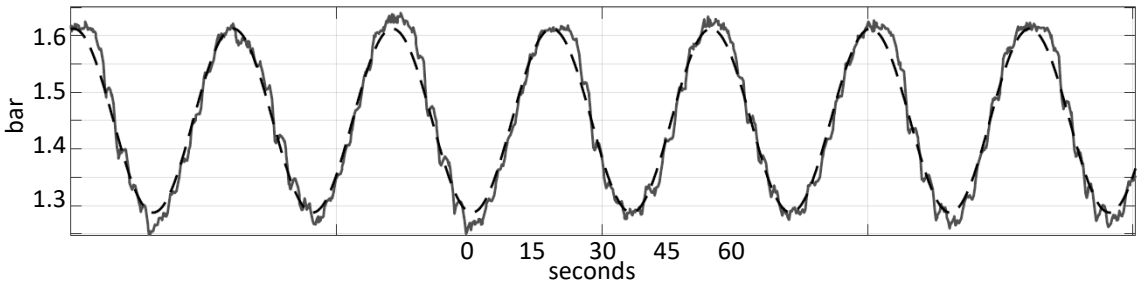

Figure 5: Time series of back pressure for sea state 5. Black dashed line indicated the reference pressure-. Solid grey line indicated the measured pressure.

For turbogenerator mapping, it is common practice to use quasi-nondimensionless variables by omitting constants c_p and d_{tg} from those in (2) and scaling other variables (for example, to use kPa instead of Pa or °C instead of K) [11]. These variables, which are used in this work include

$$\Pi_{\mathrm{tg}} = \frac{p_{\mathrm{in}}}{p_{\mathrm{out}}}, \qquad \dot{m}_{\mathrm{tg,co}} = \frac{\dot{m}_{\mathrm{tg}}\sqrt{T_{\mathrm{in}}}}{p_{\mathrm{in}}/1000}, \qquad \omega_{\mathrm{tg,co}} = \frac{\omega_{\mathrm{tg}}}{\sqrt{T_{\mathrm{in}}}},$$
$$\mathrm{T}_{\mathrm{tg}} = \frac{T_{\mathrm{in}}}{T_{\mathrm{out}}}, \qquad BSR_{\mathrm{tg}} = \frac{d_{\mathrm{tg}}\omega_{tg}}{2\sqrt{2c_pT_{\mathrm{in}}\left(1-\Pi_{\mathrm{tg}}^{1-1/\gamma}\right)}}, \qquad \upsilon_{\mathrm{tg,co}} = \frac{P_{\mathrm{tg}}}{p_{\mathrm{in}}/1000\sqrt{T_{\mathrm{in}}}}. \tag{5}$$

By rearranging these equations, it is easy to calculate the real mass flow rate and power output based on the turbogenerator speed and the inlet pressure and temperature.

Quasi-nondimensional mass flow map

To model the turbine's quasi-nondimensional mass flow map, various physics based models promulgated in the literature and compiled in [11] were trialled, but none found to produce satisfactory accuracy. One factor explaining this is the larger size of the turbine used in this experiment compared to typical automotive turbines, which are the subject of the majority of modelling efforts described in the literature. Typically, automotive turbine mass flow models are only dependent on pressure ratio. In large radial flow turbines, the centrifugal forces imparted onto the gas by the rotating turbine blades act to retard mass flow. Therefore, the turbine's rotational velocity becomes a significant factor contributing to quasi-nondimensional mass flow model accuracy.

A data-driven model consisting of a 3rd order polynomial of the form $\dot{m}_{\mathrm{tg,co}} = f_{\dot{m}}\left(\Pi_{\mathrm{tg}}, \omega_{\mathrm{tg,co}}\right)$ was developed which includes dependence on pressure ratio and quasi-nondimensional speed. Although this model cannot be used to predict turbine choking, since the polynomial fit diverges for Π_{tg} and $\omega_{\mathrm{tg,co}}$ outside of the experimental range, the safety constraints imposed by the on-board controller restrict operation in the choked region. Figure 6 shows the turbogenerator's quasi-nondimensional mass flow map with Π_{tg} and $\omega_{\mathrm{tg,co}}$ vs. $\dot{m}_{\mathrm{tg,co}}$.

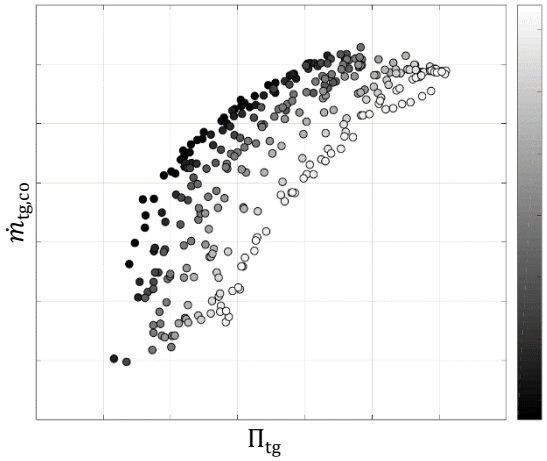

Figure 6: Quasi-nondimensional turbogenerator mass flow map. Correlation coefficient of 3rd order polynomial fit = 0.9866. Scales have been omitted to retain turbogenerator vendor's intellectual property.

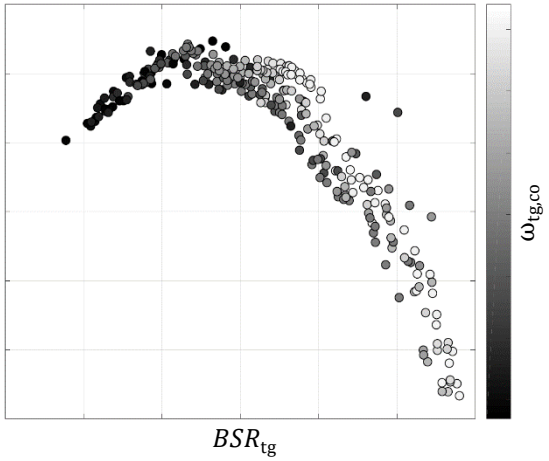

Figure 7: Turbogenerator turbine isentropic efficiency. Correlation coefficient of quadratic fit = 0.9538. Scales have been omitted to retain turbogenerator vendor's intellectual property.

Turbogenerator DC power output

The power produced by the turbogenerator's turbine and delivered to the generator is given by

$$P_{\mathrm{tg}} = \eta_{\mathrm{tg}} P_{\mathrm{tg,ideal}},$$

where η_{tg} represents the isentropic efficiency of the turbine. $P_{\mathrm{tg,ideal}}$ is the power that the turbine would produce in an ideal isentropic expansion given by

$$P_{\mathrm{tg,ideal}} = \dot{m}_{\mathrm{tg}} c_p T_{\mathrm{tg,in}} \left(1 - \Pi_{\mathrm{tg}}^{1-1/\gamma}\right).$$

Since the power extracted from the expanding exhaust gas can be calculated from experimental data using

$$P_{\mathrm{tg}} = \dot{m}_{\mathrm{tg}} c_p \left(T_{\mathrm{tg,in}} - T_{\mathrm{tg,out}}\right),$$

the isentropic efficiency is calculated from experimental data by

$$\eta_{\mathrm{tg}} = \frac{\left(T_{\mathrm{tg,in}} - T_{\mathrm{tg,out}}\right)}{T_{\mathrm{tg,in}}\left(1 - \Pi_{\mathrm{tg}}^{1-1/\gamma}\right)}.$$

To model the turbine efficiency, we follow the approach in [11] which uses a quadratic function of BSR_{tg}. Here we have used a quadratic function as well, but once which includes the dependence on $\omega_{\mathrm{tg,co}}$, as this was found to provide a superior fit. This model takes the form $\eta_{\mathrm{tg}} = f_{\eta}\left(BSR_{\mathrm{tg}}, \omega_{\mathrm{tg,co}}\right)$. Figure 7 shows the turbogenerator's isentropic efficiency map, with BSR_{tg} and $\omega_{\mathrm{tg,co}}$ vs. η_{tg}.

Having calculated P_{tg}, along with measurements of the generated DC power, $P_{\mathrm{tg,gen}}$, we can determine the losses due to mechanical friction within the turbogenerator and due to the combined electrical conversion efficiency of the generator and power electronics. Figure 8 shows the plot of P_{tg} vs. $P_{\mathrm{tg,gen}}$, with a line of best fit given by

$$P_{\mathrm{tg,gen}} = \eta_{\mathrm{gen}}\left(P_{\mathrm{tg}} - P_{\mathrm{tg},0}\right),$$

where η_{gen} is the combined mechanical and electrical efficiency and $P_{\mathrm{tg},0}$ represents the minimum power delivered to the generator before power begins to be exported. This point coincides with the minimum rectified voltage required by the power electronics before becoming active.

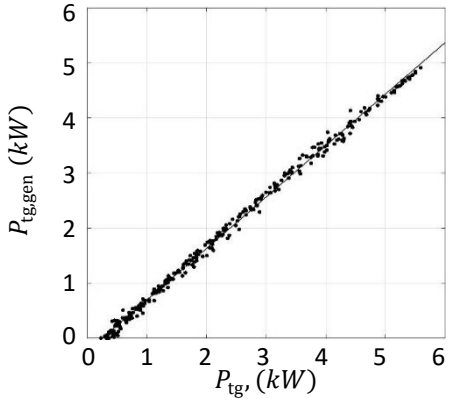

Figure 8: Turbogenerator power map

Wastegate valve mass flow

The model for the wastegate valve's mass flow rate is the same as the back pressure valve's, but uses different coefficients in $A_{\mathrm{eff}}(\theta_{\mathrm{wgv}})$.

INTERACTION BETWEEN EMPC CONTROLLER, ENGINE SIMULATION AND TEST RIG

There are numerous interactions between the simulated engine, the test rig and the EMPC controller. The EMPC controller provides control inputs for the simulated engine's fuelling rate $\dot{m}_{\mathrm{f}}$, the load on the engine τ_{l} (collected into the vector $\mathbf{u_e} = [\dot{m}_{\mathrm{f}}, \tau_{\mathrm{l}}]$), and the turbogenerator speed setpoint u_{tg} and the wastegate valve position u_{wgv} (collected into the vector $\mathbf{u_{tg}} = [u_{\mathrm{tg}}, u_{\mathrm{wgv}}]$).

The EMPC controller also requires state feedback from the simulated engine and test rig. For the engine, the states include the engine speed ω_{e}, turbocharger speed ω_{t}, and the pressures $p_{(\cdot)}$ and temperatures $T_{(\cdot)}$ in the intercooler $(\cdot)_{\mathrm{ic}}$ and cylinder block $(\cdot)_{\mathrm{cc}}$ inlet manifold $(\cdot)_{\mathrm{im}}$ and exhaust manifolds $(\cdot)_{\mathrm{em}}$. These are collected into the vector $\mathbf{x}_{\mathrm{e}} = [\omega_{\mathrm{e}}, \omega_{\mathrm{t}}, T_{\mathrm{ic}}, T_{\mathrm{cc}}, T_{\mathrm{em}}, p_{\mathrm{ic}}, p_{\mathrm{cc}}, p_{\mathrm{em}}]$. For the turbogenerator and wastegate valve, the states include turbogenerator speed ω_{tg}, turbogenerator inlet pressure p_{tg} and temperature T_{tg} and the wastegate valve position x_{wgv}. These are collected into the vector $\mathbf{x}_{\mathrm{tg}} = [\omega_{\mathrm{tg}}, x_{\mathrm{egv}}, T_{\mathrm{tg}}, p_{\mathrm{tg}}]$. In addition, the EMPC controller also requires the generated back-pressure, and for the cost function, the turbogenerator exported DC power and the exhaust temperature. The engine simulation also requires the mass flow rate through the wastegate valve to calculate the exhaust manifold pressure and temperature.

Since the air supplied by the air processing plant is substantially less than typical exhaust manifold temperatures, the control inputs to the turbogenerator, as well as the feedback to the EMPC controller and the simulated engine must be scaled accordingly. This scaling is accomplished using quasi-nondimensional variables, since these variables remain invariant between the EMPC - engine simulation and the test rig. In the following, we

denote simulated and scaled measured quantities with a hat ($\widehat{\ }$) and unscaled measured quantities without.

Exhaust temperature

The simulated exhaust temperature is calculated using both the simulated turbocharger turbine and adjusted turbogenerator's mass flow rate and outlet temperature. The simulated exhaust temperature, $\hat{T}_{\mathrm{ex}}$ is given by

$$\hat{T}_{\mathrm{ex}} = \frac{\hat{\dot{m}}_{\mathrm{t}}\hat{T}_{t} + \hat{\dot{m}}_{\mathrm{tg}}\hat{T}_{\mathrm{tg,out}}}{\hat{\dot{m}}_{\mathrm{t}} + \hat{\dot{m}}_{\mathrm{tg}}}.$$

To convert the measured $\dot{m}_{\mathrm{tg}}$ to the scaled $\hat{\dot{m}}_{\mathrm{tg}}$ for use within the simulation and control environments, the quasi-nondimensional mass flow rates are equated, and then solved for $\hat{\dot{m}}_{\mathrm{tg}}$. This yields

$$\hat{\dot{m}}_{\mathrm{tg,co}} = \dot{m}_{\mathrm{tg,co}} \Rightarrow \frac{\dot{m}_{\mathrm{tg}}\sqrt{T_{\mathrm{in}}}}{p_{\mathrm{in}}/1000} = \frac{\hat{\dot{m}}_{\mathrm{tg}}\sqrt{\hat{T}_{\mathrm{in}}}}{\hat{p}_{\mathrm{in}}/1000} \Rightarrow \hat{\dot{m}}_{\mathrm{tg}} = \frac{\hat{p}_{\mathrm{in}}\sqrt{T_{\mathrm{in}}}}{p_{\mathrm{in}}\sqrt{\hat{T}_{\mathrm{in}}}}\,\dot{m}_{\mathrm{tg}},$$

where $(\cdot)_{\mathrm{in}}$ indicates the turbogenerator inlet conditions. To convert the measured $T_{\mathrm{tg,out}}$ to the scaled $\hat{T}_{\mathrm{tg,out}}$ for use within the simulation and control environments, the temperature ratios are equated, and then solved for $\hat{T}_{\mathrm{tg,out}}$. This yields

$$\mathrm{T}_{\mathrm{tg}} = \hat{\mathrm{T}}_{\mathrm{tg}} \Rightarrow \frac{T_{\mathrm{in,tg}}}{T_{\mathrm{out,tg}}} = \frac{\hat{T}_{\mathrm{in,tg}}}{\hat{T}_{\mathrm{out,tg}}} \Longrightarrow \hat{T}_{\mathrm{out,tg}} = \frac{\hat{T}_{\mathrm{in,tg}}}{T_{\mathrm{in,tg}}}T_{out,tg},$$

Turbogenerator speed set point and feedback

The EMPC controller provides a set point to the turbogenerator, $u_{\mathrm{tg,mpc}}$. This is then converted to a quasi-nondimensional speed setpoint, $u_{\mathrm{tg,co}}$ using the MPC's internal model of the turbogenerator inlet temperature, and then back into an actual speed setpoint for the turbogenerator using the rig's turbogenerator inlet temperature as

$$u_{\mathrm{tg,co}} = \frac{u_{\mathrm{tg,mpc}}}{\sqrt{\hat{T}_{\mathrm{in}}}} = \frac{u_{\mathrm{tg}}}{\sqrt{T_{\mathrm{in}}}} \Longrightarrow u_{\mathrm{tg}} = \sqrt{\frac{T_{\mathrm{in}}}{\hat{T}_{\mathrm{in}}}}\,u_{\mathrm{tg,mpc}}.$$

Similarly, the actual turbogenerator speed is fed back into the MPC controller and simulated engine model using

$$\omega_{\mathrm{tg,mpc}} = \sqrt{\frac{\hat{T}_{\mathrm{in}}}{T_{\mathrm{in}}}}\,\omega_{\mathrm{tg}}.$$

Turbogenerator power

The DC power generated by the turbogenerator, $P_{\mathrm{tg,gen}}$ is scaled for use by the EMPC controller by equating the quasi-nondimensional power of the test rig, $\upsilon_{\mathrm{tg,co}}$, to the EMPC quasi-nondimensional power in the controller and simulation environment, $\hat{\upsilon}_{\mathrm{tg,co}}$, and solving for $\hat{P}_{\mathrm{tg,gen}}$. This yields

$$\upsilon_{\mathrm{tg,co}} = \hat{\upsilon}_{\mathrm{tg,co}} \Rightarrow \frac{P_{\mathrm{tg,gen}}}{p_{\mathrm{in}}/1000\sqrt{T_{\mathrm{in}}}} = \frac{\hat{P}_{\mathrm{tg,gen}}}{\hat{p}_{\mathrm{in}}/1000\sqrt{\hat{T}_{\mathrm{in}}}} \Rightarrow \hat{P}_{\mathrm{tg,gen}} = \frac{\hat{p}_{\mathrm{in}}\sqrt{\hat{T}_{\mathrm{in}}}}{p_{\mathrm{in}}\sqrt{T_{\mathrm{in}}}}P_{\mathrm{tg,gen}}.$$

CONCLUSION & FUTURE WORK

This paper describes the turbogenerator test rig used to map the performance of the turbogenerator, as well as serving as a platform to test an EMPC controller using hardware-

in-the-loop simulations. The control of the air flow through the rig to reproduce wave induced back-pressure fluctuations and engine operating conditions is described. Furthermore, the methodology of integrating the test rig into the simulation environment is outlined.

The future work enabled by the HIL simulations on the test rig includes verifying the efficacy of the EMPC controller for both submarine and surface vessel applications, determining the engine/turbogenerator configurations most suitable to these applications, and exploring the trade-off between the controller performance and computational complexity. These studies all aim to find a combination of system and controller design parameters which maximise the energy efficiency of diesel engines while ensuring all other system performance objectives are met.

REFERENCES

[1] N. Olshina, C. Manzie, M. Brear, P. Hield, O. Tregenza, "Waste Heat Recovery of Marine Diesel Engines," *in Pacific 2017, International Maritime Conference*, 2012.

[2] D. V. Singh and E. Pedersen, "A review of waste heat recovery technologies for maritime applications," *Energy Convers. Manag.*, vol. 111, pp. 315–328, 2016.

[3] P. Hield, "The effect of back pressure on the operation of a diesel engine," Australian Government Department of Defence - Defence Science and Technology Organisation, Technical Report DSTO-TR-2531, 2011.

[4] MAN Diesel & Turbo, "Waste Heat Recovery System (WHRS) for Reduction of Fuel Consumption, Emissions and EEDI".

[5] T.J. Broomhead, C. Manzie, P. Hield, and M.J. Brear, "An experimental investigation of additional actuators on a submarine diesel generator," *Control Eng. Pract.*, vol. 55, pp. 26–37, Oct. 2016.

[6] T.J. Broomhead, C. Manzie, P. Hield, R.C. Shekhar, and M.J. Brear, "Economic model predictive control and applications for diesel generators," *IEEE Trans. Control Syst. Technol.*, vol. 25, no. 2, pp. 388–400, 2016.

[7] N. Olshina, C. Manzie, P. Hield and M. Brear, "A Framework for Robust Nonlinear Economic MPC Without Terminal Constraints for a Class of Time Varying Systems," *2018 15th International Conference on Control, Automation, Robotics and Vision (ICARCV)*, Singapore, 2018, pp. 668-673.

[8] V. Bachtiar, C. Manzie, W.H. Moase, E.C. Kerrigan,"Analytical results for the multi-objective design of model-predictive control," *Control Engineering Practice,* 56:1-12, 2016.

[9] F.M. White, "*Fluid Mechanics*", 8th ed., McGraw Hill, 2016

[10] L. Guzzella, C.H. Onder, "*Introduction to Modeling and Control of Internal Combustion Engine Systems*," 2nd ed., Springer, 2010.

[11] L. Eriksson and L. Nielsen, *Modeling and Control of Engine and Drivelines*, 1st ed., Wiley, 2014.